

Thermomechanical Properties of Poly(methyl methacrylate)s Containing Tethered and Untethered Polyhedral Oligomeric Silsesquioxanes

Edward T. Kopesky,[†] Timothy S. Haddad,[‡] Robert E. Cohen,^{*,†} and Gareth H. McKinley^{*,§}

Department of Chemical Engineering, Massachusetts Institute of Technology, Cambridge, Massachusetts 02139; ERC Inc., Air Force Research Laboratory, Edwards AFB, California 93524; and Department of Mechanical Engineering, Massachusetts Institute of Technology, Cambridge, Massachusetts 02139

Received May 28, 2004; Revised Manuscript Received August 23, 2004

ABSTRACT: Poly(methyl methacrylate)s (PMMA) containing both tethered and untethered polyhedral oligomeric silsesquioxanes (POSS) were examined through the use of wide-angle X-ray diffraction (WAXD), differential scanning calorimetry (DSC), and rheological characterization. The presence of tethered-POSS in entangled copolymers leads to a decrease in the plateau modulus (G_N^0) when compared with PMMA homopolymer. Two untethered-POSS fillers, cyclohexyl-POSS and isobutyl-POSS, were blended with PMMA homopolymer. Both DSC and rheological results suggest a regime at low untethered-POSS loadings ($\phi \leq 0.05$) in PMMA in which much of the POSS filler resides in the matrix in a nanoscopically dispersed state. This well-dispersed POSS decreases the zero-shear-rate viscosity (η_0). Above this regime, an apparent solubility limit is reached, and beyond this point additional untethered-POSS aggregates into crystallites in the PMMA matrix. These crystallites cause both the viscosity and the plateau modulus to increase in a way consistent with classical predictions for hard-sphere-filled suspensions. The principles of time-temperature superposition are followed by these nanocomposites; however, fits to the WLF equation show no strong trend with increasing POSS loading. Isobutyl-POSS was also blended with a POSS-PMMA copolymer containing 25 wt % tethered isobutyl-POSS distributed randomly along the chain. Blends of untethered-POSS with copolymer show a significant increase in η_0 for all loadings, greater than that expected for traditional hard-sphere fillers. This is a result of associations between untethered-POSS and tethered-POSS cages in the blend, which retard chain relaxation processes in a way not observed in either the homopolymer blends or the unfilled copolymers. Time-temperature superposition also holds for the filled copolymer system, and these blends show a strong increase in the WLF coefficients, suggesting that both free volume and viscosity increase with filler loading.

Introduction

Polyhedral oligomeric silsesquioxanes (POSS)¹ have drawn considerable interest due to their hybrid organic-inorganic structure which consists of a silica cage with organic R groups on the corners.^{2–5} A generic POSS molecule ($R_8Si_8O_{12}$) is shown at the top of Figure 1. When covalently tethered to a polymer backbone, POSS has been shown to improve the thermooxidative stabilities of polymers,⁶ increase their glass transition temperatures,^{7–9} lower their zero-shear-rate viscosities,¹⁰ and increase the toughness of homopolymer blends.¹¹ POSS may be incorporated into a polymer matrix in two primary ways: chemically tethered to the polymer or as untethered filler particles, both of which are shown in Figure 1. (For brevity, we will at times denote these limits as CO and F, respectively, to denote POSS copolymer and POSS filler.) In the copolymer case, one corner of the POSS macromer is functionalized, allowing it to be grafted onto the polymer backbone. Untethered POSS filler differs in that all corners of the cages have the same R group and are nonreactive. The edges of the ternary composition diagram shown in Figure 1 indicate that there are three types of binary blends to consider: untethered POSS may be blended with either the homopolymer, poly(methyl methacrylate) (PMMA) in

this case, or with a tethered-POSS-containing copolymer, which in this study has a PMMA backbone. The homopolymer and the copolymer may also be blended together. The interior of the triangular diagram represents the variety of ternary compositions that can be formulated. The present study focuses exclusively on the filler-homopolymer (F/HP) and the filler-copolymer (F/CO) sides of the composition space in order to discern systematic differences, both quantitative and qualitative, between the thermomechanical properties of these two binary blend systems. The ranges of composition studied are indicated by the two arrows in Figure 1.

A key factor in optimizing the properties of a POSS-polymer system is the thermodynamic interaction between the pendant R group and the matrix. This controls the degree of dispersion of POSS in the matrix and thus the degree of property modification. Untethered POSS particles can disperse on a molecular scale (~ 1.5 nm) or as crystalline aggregates which can be on the order of microns in size.¹² An important question is whether both of these states of dispersion exist simultaneously, and to varying degrees, in a given POSS-polymer blend. Additional morphologies are possible when tethered-POSS particles are present. Their covalent attachment to the polymer backbone limits the length scale of association and, at high volume fractions, has been shown to lead to two-dimensional raftlike structures¹³ which are shaped similarly to clay platelets.¹⁴

[†] Department of Chemical Engineering, MIT.

[‡] ERC Inc.

[§] Department of Mechanical Engineering, MIT.

* Corresponding authors. E-mail: recohen@mit.edu; gareth@mit.edu.

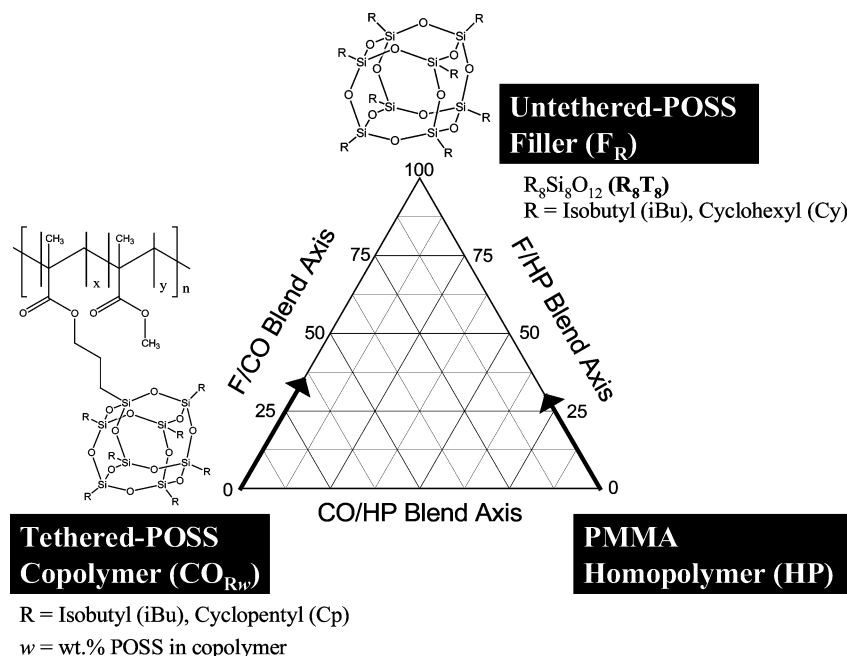


Figure 1. Ternary composition diagram for untethered-POSS filler (F), tethered-POSS containing copolymer with PMMA backbone (CO), and PMMA homopolymer (HP). The arrows represent the ranges of composition (in volume percent filler) analyzed in the present study.

Rheological characterization is an important tool for comparing behavior of the F/HP and the F/CO blend systems. Previous work on POSS rheology has been scarce, with few relevant publications.^{10,15} In a study by Romo-Uribe et al.,¹⁰ poly(methylstyrenes) containing two different types of tethered-POSS [R = cyclopentyl (0–63 wt %) and R = cyclohexyl (0–64 wt %)] were tested in small-amplitude oscillatory shear flow. One notable result was the appearance of a rubbery plateau ($\sim 10^3$ Pa) in the storage modulus G' at low frequencies for the 42 wt % cyclohexyl-POSS copolymer, indicating formation of a percolated network by the tethered-POSS particles. Low-frequency plateaus in G' were not observed for copolymers containing 27 wt % cyclohexyl-POSS or 45 wt % cyclopentyl-POSS. For the 42 wt % cyclohexyl-POSS copolymer of molecular weight $M_w = 120\,000$ g/mol and degree of polymerization $x_w = 420$, the viscosity was approximately half that of the homopolymer, which had M_w and x_w values of only 34 000 g/mol and 180, respectively. The study of Romo-Uribe et al. used only unentangled to very mildly entangled polymers, so no detailed information on plateau moduli and hence entanglement molecular weight (M_e) of the copolymers could be obtained.

The rheological properties of blends of homopolymers and untethered-POSS were investigated by Fu et al.¹⁵ for ethylene–propylene copolymer containing 0, 10, 20, and 30 wt % methyl-POSS. At high frequencies, for loadings up to 20 wt %, the storage modulus G' remained essentially unchanged, only diverging at low frequencies, where a plateau of increasing magnitude (10^2 – 10^3 Pa) formed at high POSS loadings. Viscometric tests showed that the viscosity of the unfilled polymer and the 10 wt % filled blend were virtually the same over a shear rate range of 10^{-4} – 10^{-1} s $^{-1}$, while the viscosities of the 20 and 30 wt % blends were substantially higher over the same shear rate range. No information on rheological behavior at POSS loadings below 10 wt % was reported.

Studies of other (non-POSS) nanoparticles have demonstrated the unusual effect that very small (~ 10 nm)

nanoparticles have on polymer matrices.^{16,17} In the work of Zhang and Archer,¹⁶ poly(ethylene oxide) was filled with two types of 12 nm silica particles. In one case, the particles received no surface treatment, allowing them to hydrogen bond with the polymer matrix. Predictably, a dramatic enhancement in the linear viscoelastic properties was seen at very small loadings, with a low-frequency plateau in the storage modulus G' appearing at a very small volume loading of particles $\phi \approx 0.02$. However, when the particles were treated with a PEO-like organosilane, there was virtually no difference between the linear viscoelastic properties of the PEO and a 2 vol % blend. In fact, the loss moduli G'' were virtually indistinguishable between the two samples in the terminal flow region, giving identical zero-shear-rate viscosities η_0 from linear viscoelasticity theory. This result suggests that polymers filled with very small nanoparticles ($d \sim 10$ nm) with weak polymer–filler interactions do not follow the classical theory for hard-sphere-filled suspensions:¹⁸

$$\eta_0(\phi) = \eta_0(0)\{1 + 2.5\phi + \dots\} \quad (1)$$

where ϕ is the particle volume fraction, which predicts a monotonic increase in viscosity with particle loading. This was further established by Mackay et al.,¹⁷ who filled linear polystyrene melts with highly cross-linked 5 nm polystyrene nanoparticles. A substantial decrease in viscosity—more than 50% for some compositions—was reported, but no consistent trend in viscosity with increasing particle loading was found. The drop in viscosity was attributed to an increase in free volume and a change in conformation of the polystyrene chains in the matrix, although the precise mechanisms for these effects are still not well understood.¹⁹

The present study seeks to determine whether nano-filled polymer systems containing untethered-POSS filler and tethered-POSS groups demonstrate similar unusual flow phenomena. The POSS nanoparticle–matrix interaction is different from those mentioned above in that there is the potential for molecularly

Table 1. Polymers Used in the Study

polymer name	POSS type	wt % POSS	mol % POSS	M_w (g/mol)	PDI	α_w
HP		0	0	80 200	1.68	800
HP2		0	0	260 000	1.89	2600
CO _{iBu15}	isobutyl	15	2.1	205 000	2.26	1740
CO _{iBu25}	isobutyl	25	3.4	62 700	1.73	490
CO _{2iBu25}	isobutyl	25	3.4	560 000	2.64	4350
CO _{Cp25}	cyclopentyl	25	3.2	20 000	3.21	5590

dispersed nanoparticles, crystalline filler aggregates, and, in the filled copolymer case, nanoscopic POSS domains containing associated tethered- and untethered-POSS groups. The combined effect of these states of dispersion is addressed in the present study.

Experimental Section

Synthesis of High Molecular Weight Polymers. The POSS (R)₇Si₈O₁₂(propyl methacrylate) monomers, with R = isobutyl and cyclopentyl, were either synthesized according to existing literature procedures²⁰ or obtained from Hybrid Plastics (Fountain Valley, CA). Toluene (Fisher) was dried by passage through an anhydrous alumina column, vacuum-transferred, and freeze–pump–thawed three times prior to use. Methyl methacrylate (Aldrich) was passed through an inhibitor-removal column (Aldrich), freeze–pump–thawed twice, vacuum-transferred to a collection vessel, and stored at –25 °C in a glovebox under nitrogen. AIBN free radical initiator (TCI) was used as received. NMR spectra were obtained on a Bruker 400 MHz spectrometer and referenced to internal chloroform solvent (¹H and ¹³C) or external tetramethylsilane (²⁹Si).

In a 500 mL jacketed reactor, (isobutyl)₇Si₈O₁₂(propyl methacrylate) (40.0 g, 0.0424 mol), methyl methacrylate (120.0 g, 1.199 mol), 0.25 mol % AIBN (0.509 g, 3.10 mmol), and toluene (124 mL) were loaded under a nitrogen atmosphere to produce the isobutyl-POSS copolymer CO_{iBu25}. The jacketed part of the reactor was filled with heating fluid maintained at 60 °C, and the reaction mixture was stirred under a nitrogen atmosphere. Overnight the solution became very viscous. After 40 h, the reactor was opened to air, diluted with CHCl₃ (200 mL), and allowed to stir overnight to form a less viscous solution. This was slowly poured through a small bore funnel into well-stirred methanol. A fibrous polymer was formed around the stir bar. After the addition was complete, the polymer was stirred for another hour before it was removed from the methanol/toluene mixture and dried overnight at 40 °C under vacuum. A nearly quantitative yield of 158.1 g of copolymer was isolated. A ¹H NMR spectrum was obtained to show that no residual unreacted POSS monomer was present (demonstrated by the absence of any peaks in the 5–6.5 ppm olefin region of the spectrum). Integration of the ¹H NMR spectra indicated that the mol % POSS in the copolymer (3.4 mol %) was the same as the % POSS in the monomer feed. The same synthesis procedure was used to produce the cyclopentyl version of the copolymer (CO_{Cp25}) and the high molecular weight homopolymer (HP2). The amounts of reagents used to synthesize CO_{Cp25} were as follows: (cyclopentyl)₇Si₈O₁₂(propyl methacrylate) (40.0 g, 0.0389 mol), methyl methacrylate (120.0 g, 1.199 mol), 0.25 mol % AIBN (0.508 g, 3.09 mmol), and toluene (124 mL). A yield of 156.1 g of copolymer was isolated. ¹H NMR spectra confirmed that the copolymer was monomer-free and that the mol % POSS in the copolymer (3.1 mol %) was the same as the % POSS in the monomer feed. The amounts of reagents used to synthesize the homopolymer HP2 were as follows: methyl methacrylate (125.0 g, 1.249 mol), 0.25 mol % AIBN (0.513 g, 3.12 mmol), and toluene (125 mL). A yield of 123.4 g of homopolymer was isolated. ¹H NMR spectra confirmed that the homopolymer was monomer-free. Molecular weight (M_w) and polydispersity (PDI) values for the copolymers and the homopolymer (Table 1) were determined using a Waters gel permeation chromatograph (GPC) on a polystyrene standard with THF as eluent.

Additional Materials. A commercial PMMA resin from Atofina Chemicals (Atoglas V920, HP) was used for homopoly-

mer blends due to its stability at high temperatures. A copolymerized PMMA containing 15 wt % tethered isobutyl-POSS (CO_{iBu15}) was purchased from Hybrid Plastics. A PMMA copolymer containing 25 wt % tethered isobutyl-POSS (CO_{iBu25}) was purchased from Sigma-Aldrich for use in blend characterization. Molecular weight and polydispersity values for these polymers are reported in Table 1.

Two different POSS fillers [isobutyl-POSS (F_{iBu}) and cyclohexyl-POSS (F_{Cy})] were purchased from Hybrid Plastics. The molecular weights of these fillers are 873.6 and 1081.9 g/mol, respectively. The crystalline density of cyclohexyl-POSS was reported to be 1.174 g/cm³ by Barry et al.²¹ The value for isobutyl-POSS has not been reported, but Larsson reported crystal densities for many POSS cages with similar structure and an estimate of 1.15 g/cm³ was deemed a reasonable value for the isobutyl-POSS.²² The density of the PMMA homopolymer HP was 1.17 g/cm³.

Blend Preparation. Each of the filler species (cyclohexyl-POSS and isobutyl-POSS) was blended separately with the PMMA homopolymer HP in a DACA Instruments microcompounder at 220 °C for 5 min at compositions between 1 and 30 vol %. The isobutyl-POSS was also blended with the low molecular weight isobutyl-POSS copolymer CO_{iBu25} at 175 °C for 5 min at compositions between 2 and 35 vol %; the lower temperature was required to minimize thermal degradation of the copolymer. Rheological samples were made by compression-molding the extruded samples into disks 25 mm in diameter with a thickness of 2 mm. Molding temperatures were 190 °C for the homopolymer blends and 150 °C for the copolymer blends.

X-ray Scattering. Wide-angle X-ray diffraction (WAXD) was carried out on two different diffractometers. Room temperature tests were performed on a Rigaku RU300 18 kW rotating anode generator with a 250 mm diffractometer. Tests at room temperature and at an elevated temperature were performed in a Siemens 2D small-angle diffractometer configured in Wide-angle mode using a 12 kW rotating anode; these samples (powders mounted on Kapton tape) were tested in transmission. Cu K α radiation was used in both cases.

Differential Scanning Calorimetry (DSC). Thermal analysis was performed on a TA Instruments Q1000 DSC. Samples were heated at 5 °C/min and cooled at the same rate, and then data were collected on the second heating ramp at the same heating rate. Glass transition temperatures (T_g) were determined from the inflection point in the heat flow vs temperature curves. Melting points (T_m) and latent heats ($\Delta H/g_{POSS}$) of the isobutyl-POSS-filled homopolymer blends were determined from the peak and the area of each endotherm, respectively.

Rheological Characterization. Rheological tests were performed on two separate rheometers. Linear viscoelastic tests on the high molecular weight homopolymer (HP2) and the high molecular weight copolymers (CO_{iBu15}, CO_{2iBu25}, and CO_{Cp25}) were performed on a Rheometrics RMS-800 strain-controlled rheometer at strains between 0.1 and 1% and at temperatures between 140 and 220 °C. All blend samples were rheologically characterized using a TA Instruments AR2000 stress-controlled rheometer. The filler–homopolymer blends were tested between 140 and 225 °C; the filler–copolymer blends were tested between 120 and 170 °C. All rheology samples were tested in air using 25 mm parallel plates with gap separations of approximately 2 mm.

Results

Characterization. X-ray diffraction patterns taken at room temperature for the cyclohexyl-POSS-filled

Table 2. Quantitative Melting Behavior of Isobutyl-POSS-filled PMMA

blend	T_m^1 (°C)	ΔH_1 (J/g _{POSS})	T_m^2 (°C)	ΔH_2 (J/g _{POSS})	$\Delta H_1/\Delta H_1^*$	$\Delta H_2/\Delta H_2^*$
2.5F _{iBu} /97.5HP	51	1.34		0.00	0.11	0.00
5F _{iBu} /95HP	53	3.18	255	3.26	0.27	0.20
10F _{iBu} /90HP	54	4.90	263	11.4	0.42	0.71
30F _{iBu} /70HP	58	7.46	266	12.3	0.63	0.76
100F _{iBu}	60	11.8	261	16.1	1.00	1.00

homopolymer (F_{Cy}/HP) and the isobutyl-POSS-filled copolymer (F_{iBu}/CO1_{iBu}25) blend systems are shown in Figure 2. From Figure 2a it is clear that even at the

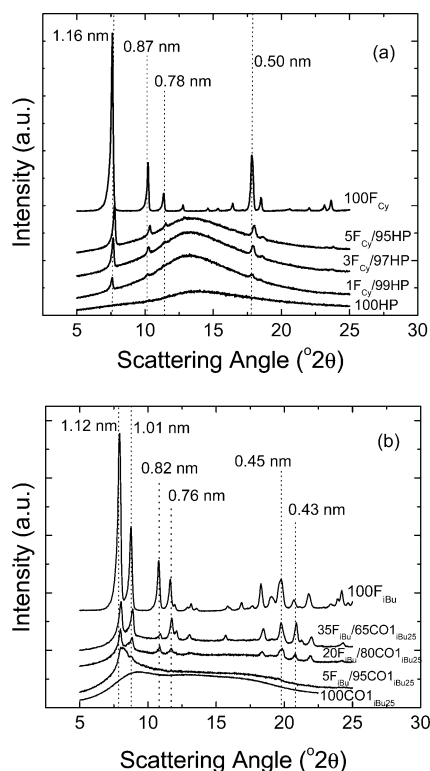


Figure 2. WAXD patterns for blends composed of (a) cyclohexyl-POSS in PMMA homopolymer and (b) isobutyl-POSS in copolymer containing 25 wt % isobutyl-POSS on the chain (CO1_{iBu}25).

lowest loading of 1 vol % filler (1F_{Cy}/99HP) appreciable POSS crystallinity is present in the homopolymer blends. There is strong correspondence between the peak patterns of the blends and that of the pure POSS powder, and the peak locations agree with the results of Barry et al.²¹ for cyclohexyl-POSS to within 0.01 nm. Sharp crystalline peaks were also observed at room temperature in the isobutyl-POSS-filled homopolymer blend system (F_{iBu}/HP) for all blend compositions.

The WAXD pattern for the copolymer CO1_{iBu}25 in Figure 2b shows only a slight hump at $2\theta = 9.1^\circ$ ($d = 0.97$ nm). The absence of sharp peaks is consistent with previous WAXD studies of polymers containing tethered-POSS at comparable weight fractions.^{10,13} At 5 vol % isobutyl-POSS, a broad peak forms which spans the 2θ range of the two highest peaks in the POSS powder spectrum ($7.5^\circ < 2\theta < 9^\circ$). At higher loadings, the peak pattern closely resembles that of the POSS powder. On the basis of sharper line widths in the spectrum of the 5 vol % cyclohexyl-POSS-filled homopolymer (5F_{Cy}/95HP) compared to those in the 5% isobutyl-POSS-filled copolymer (5F_{iBu}/95CO1_{iBu}25), it is clear that at low filler loadings there are substantially larger POSS crystals in the homopolymer blend. While the relative extents

of crystallinity between the two types of blends are not easily determined from WAXD, the absence of any sharp peaks in the 5F_{iBu}/95CO1_{iBu}25 blend indicates better nanodispersion of untethered-POSS at low loadings in the filled copolymer blend system compared to the filled homopolymer systems.

The melting behavior of the blends was quantified using DSC, and representative curves for the isobutyl-POSS-filled homopolymer system (F_{iBu}/HP) are reproduced in Figure 3. In the pure isobutyl-POSS filler

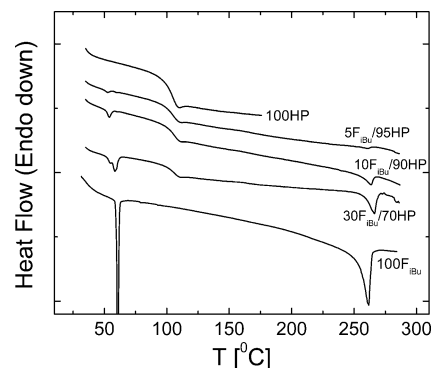


Figure 3. DSC curves for PMMA homopolymer filled with isobutyl-POSS. Two distinct endotherms are apparent in the more highly filled samples, with the size of the endotherms proportionally larger at higher loadings.

(100F_{iBu}), there are two endotherms: a sharp one at $T = 60^\circ\text{C}$ and a broader one at $T = 261^\circ\text{C}$. Similar results are seen in the F_{iBu}/HP blends, and the endotherms increase in magnitude with increasing POSS content. The locations and sizes of the endotherms for the F_{iBu}/HP system are reported in Table 2.

In Figure 4, we plot the heat of fusion per gram of

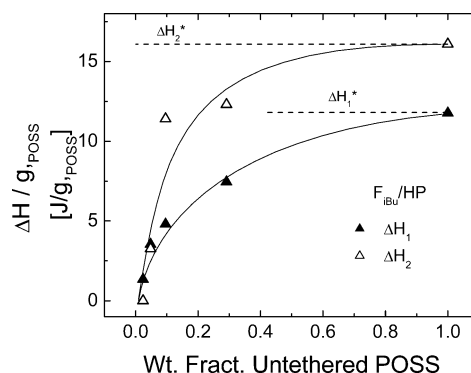


Figure 4. Heats of fusion per gram isobutyl-POSS in the sample for both thermal transitions of isobutyl-POSS-PMMA blends.

isobutyl-POSS filler in the F_{iBu}/HP samples as a function of POSS content. The horizontal dashed lines correspond to ΔH_1^* and ΔH_2^* , which are the latent heats for the isobutyl-POSS filler's low-temperature transition ($T = 60^\circ\text{C}$) and high-temperature transition ($T = 260^\circ\text{C}$), respectively. All points would fall on these lines if the isobutyl-POSS had the same degree of

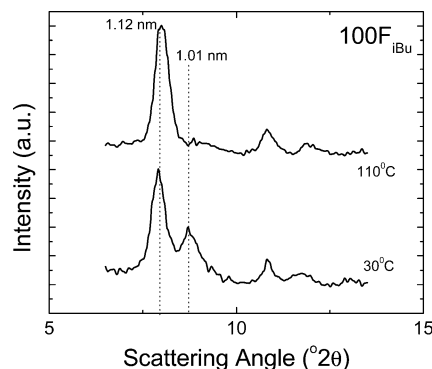


Figure 5. WAXD patterns for isobutyl-POSS powder taken below the first thermal transition of the powder (30 °C) and also above (110 °C).

Table 3. Rheological Properties of Unfilled Entangled Polymers

polymer	wt % POSS	G_N^0 (Pa) ($T_0 = 170$ °C)	M_e (g/mol)	$Z = M_w/M_e$	T_g (°C)
HP2	0	5.2×10^5	6200	43	124
CO _{iBu} 15	15	4.5×10^5	7100	29	87
CO _{2iBu} 25	25	3.4×10^5	9400	60	113
CO _{Cp} 25	25	3.7×10^5	8900	81	126

crystallinity in the blends as in its pure powder. However, the data show an increase in the heat of fusion per gram of POSS filler $\Delta H/g_{\text{POSS}}$ with increasing POSS content. The region of steepest increase is below 10 vol %. This indicates that at low loadings a large fraction of the POSS enters the polymer matrix as molecularly dispersed nanoparticles. As the concentration of filler increases, a limiting value corresponding to the pure POSS powder is approached from below. This implies that a solubility limit of POSS nanoparticles exists in the PMMA matrix. Similar results were observed for the copolymer blend system's (F_{iBu}/CO_{1iBu}25) first endotherm; however, the second endotherm of the filler ($T \sim 260$ °C) could be not be reached before extensive thermal degradation occurred. The cyclohexyl-POSS powder (F_{Cy}) showed no melting transition below 400 °C.

To determine the nature of the two endotherms in the isobutyl-POSS, the powder was heated in a sealed glass capillary from $T = 25$ °C to $T = 280$ °C. There was no apparent change in the powder until 265 °C, at which point the sample abruptly turned to liquid. Thus, the high-temperature transition corresponds to a melting point.

Additional WAXD was performed on the isobutyl-POSS to examine the thermal transition at 60 °C. A separate diffractometer equipped with a hot stage was used, and diffraction patterns taken at 30 and 110 °C are shown in Figure 5. At 30 °C two closely spaced peaks are present between $7^\circ < 2\theta < 10^\circ$. The smaller of these (at $d = 1.01$ nm) is not present in the 110 °C spectrum while the larger peak (at $d = 1.12$ nm) has a slightly increased height and breadth at 110 °C. This indicates that the thermal event at 60 °C is likely a crystal-crystal transition, which have been observed in side-chain liquid crystalline polyacetylenes²³ and in various amphiphilic salts of ammonium, phosphonium, and pyridinium.²⁴ The precise mechanism of this transition is unclear; however, it appears that the isobutyl-POSS is present in two crystal forms below 60 °C and only one above that temperature. Larsson²² reported two crystal forms for (*n*-propyl)-POSS, stating that the two forms differ in the packing of the propyl groups within the crystal.

Values of the glass transition temperature (T_g) were also obtained from the DSC curves. Table 4 shows that there was no significant change in the glass transition temperature in either filled homopolymer blend system (F_{Cy}/HP and F_{iBu}/HP) over the range of filler loadings. In the filled copolymer system (F_{iBu}/CO_{1iBu}25), whose T_g values are reported in Table 5, there was no change for volume fractions $\phi \leq 0.20$ before an 8 °C jump was observed in the 30 vol % blend.

Rheology. In Figure 6, we show master curves for the storage modulus G' and the loss tangent $\tan \delta = G''/G'$ at $T_0 = 170$ °C for four unfilled polymers: a high-molecular-weight homopolymer (HP2) and three highly entangled copolymers (CO_{iBu}15, CO_{2iBu}25, and CO_{Cp}25). The storage moduli show a significant shift downward

Table 4. WLF Parameters, Zero-Shear-Rate Viscosities, and T_g Values for Untethered-POSS-Filled Homopolymer Blends

blend composition	c_1^0	c_2^0 (K)	f_0/B ($T_0 = 190$ °C)	f_g/B ($T = T_g$)	η_0 (Pa s) ($T_0 = 190$ °C)	T_g (°C)
100HP	8.6	207	0.050	0.030	1.2×10^5	105
1F _{Cy} /99HP	8.7	208	0.050	0.030	9.6×10^4	105
3F _{Cy} /97HP	9.0	214	0.048	0.029	1.0×10^5	105
5F _{Cy} /95HP	9.0	213	0.048	0.029	1.1×10^5	106
10F _{Cy} /90HP	9.9	233	0.044	0.028	1.6×10^5	106
20F _{Cy} /80HP	7.6	176	0.057	0.030	<i>a</i>	105
30F _{Cy} /70HP ^b					<i>d</i>	106
2.5F _{iBu} /97.5HP	8.4	202	0.052	0.030	9.1×10^4	105
5F _{iBu} /95HP	8.6	205	0.051	0.030	9.2×10^4	105
10F _{iBu} /90HP	9.4	212	0.047	0.027	1.2×10^5	103
20F _{iBu} /80HP	7.4	175	0.059	0.030	<i>c</i>	105
30F _{iBu} /70HP ^b					<i>d</i>	106

^a $> 1.8 \times 10^5$ Pa s. ^b WLF fit was poor, and the coefficients are considered unreliable. ^c $> 1.9 \times 10^5$ Pa s. ^d Sample exhibited a yield stress.

Table 5. WLF Parameters, Zero-Shear-Rate Viscosities, and T_g Values for Untethered-POSS-Filled Copolymer Blends

blend composition	c_1^0	c_2^0 (K)	f_0/B ($T_0 = 135$ °C)	f_g/B	η_0 (Pa s) ($T_0 = 150$ °C)	T_g (°C)	$N_{\text{untethered}}/N_{\text{tethered-POSS}}$
100CO _{1iBu} 25	9.1	120	0.048	0.032	4.3×10^5	95	0.00
2F _{iBu} /98CO _{1iBu} 25	6.6	90	0.066	0.037	5.0×10^5	96	0.09
5F _{iBu} /95CO _{1iBu} 25	6.6	85	0.065	0.035	6.8×10^5	95	0.23
20F _{iBu} /80CO _{1iBu} 25	8.3	110	0.053	0.033	1.8×10^6	95	1.08
30F _{iBu} /70CO _{1iBu} 25 ^a					<i>b</i>	103	1.85

^a WLF fit was poor, and the coefficients are considered unreliable. ^b $> 5.0 \times 10^6$ Pa s.

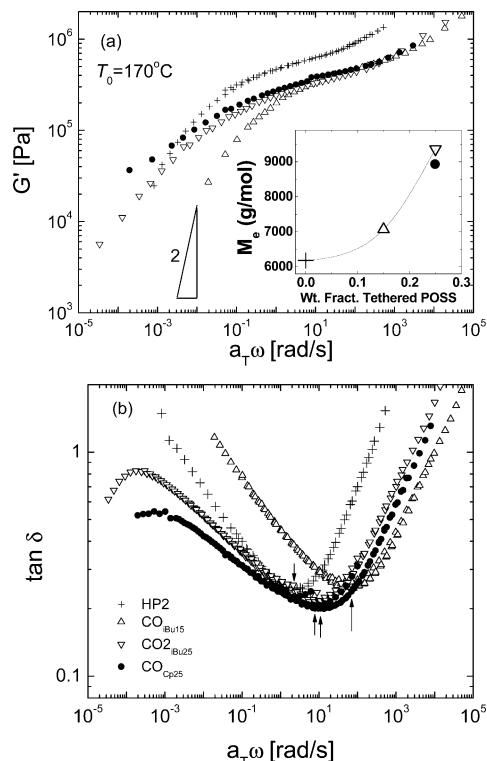


Figure 6. Master curves for (a) the storage modulus G' and (b) the loss tangent $\tan \delta = G''/G'$ for entangled copolymers containing 15 and 25 wt % tethered-POSS on a PMMA backbone. Master curves for an entangled PMMA homopolymer (HP2) are also shown. The arrows in (b) correspond to the minima in the loss tangent curves ($T_0 = 170^\circ\text{C}$).

and to the right with the addition of POSS to the chain. The magnitude of the storage modulus is similar for all three copolymers even though they exhibit significantly different glass transition temperatures (Table 3) that bracket the T_g of the homopolymer. Approximate plateau moduli (G_N^0) were calculated using the convention^{25,26}

$$G_N^0 = (G'(\omega))_{\tan \delta \rightarrow \min} \quad (2)$$

where the plateau modulus is taken as the point in the storage modulus where the loss tangent $\tan \delta = G''/G'$ passes through a minimum. These minima are noted by the arrows in Figure 6b. Values of the entanglement molecular weight, M_e , were then calculated from the expression²⁷

$$M_e = \left(\frac{4}{5}\right) \frac{\rho RT}{G_N^0} \quad (3)$$

These values are tabulated in Table 3 along with $Z = M_w/M_e$, the number of entanglements per chain. The plateau modulus for PMMA ($G_N^0 = 5.2 \times 10^5$ Pa) at $T_0 = 170^\circ\text{C}$ agrees with the values reported in Fuchs et al.,²⁸ which ranged from $4.6 \times 10^5 \leq G_N^0 \leq 6.1 \times 10^5$ Pa at $T_0 = 190^\circ\text{C}$. The data reported by Fuchs et al. were for monodisperse PMMAs with the exception of the sample with the lowest plateau modulus, which was for a PMMA with a polydispersity $\text{PDI} = 2.0$, similar to that for HP2 in this study. The terminal region and zero-shear-rate value of the viscosity for these PMMA copolymers could not be readily accessed due to thermal instability at high temperatures: HP2, $\text{CO}_{i\text{Bu}15}$, and

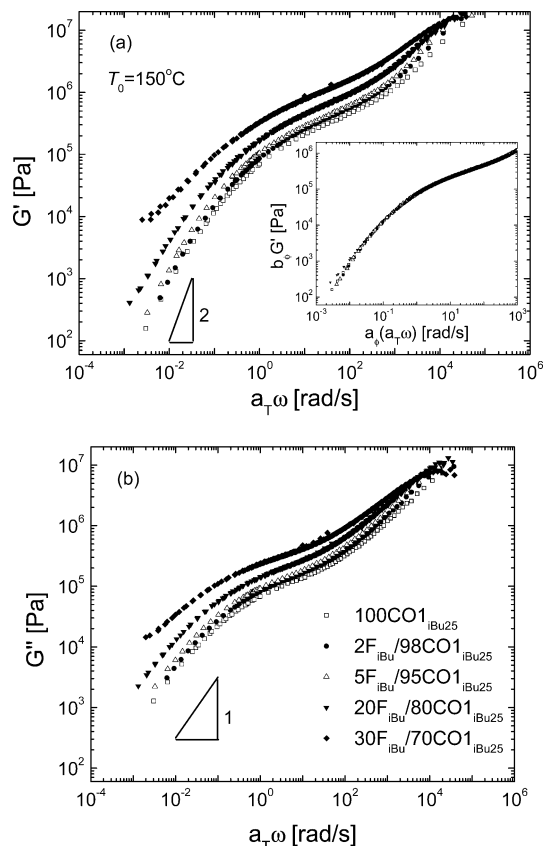


Figure 7. Master curves for (a) the storage modulus and (b) the loss modulus for blends of isobutyl-POSS at between 0 and 30 vol % in a copolymer containing 25 wt % isobutyl-POSS on the chain ($\text{CO1}_{i\text{Bu}25}$) ($T_0 = 150^\circ\text{C}$).

$\text{CO2}_{i\text{Bu}25}$ all depolymerized at temperatures above 200°C , leading to foaming of the samples; $\text{CO}_{\text{Cp}25}$ cross-linked above 200°C , causing a low-frequency plateau in the storage modulus G' and rendering the sample insoluble in THF.

The poor thermal stability of these polymers for extended times at high temperature led to the use of different matrix materials for the blend portion of the study. In particular, a copolymer ($\text{CO1}_{i\text{Bu}25}$) with substantially lower molecular weight (see Table 1) was used to study the effect of blending isobutyl-POSS filler with copolymer. In Figure 7, we show linear viscoelastic moduli for blends of isobutyl-POSS and copolymer ($\text{FiBu}/\text{CO1}_{i\text{Bu}25}$) at a reference temperature $T_0 = 150^\circ\text{C}$ for filler loadings between 0 and 30 vol %. The storage and loss moduli G' and G'' increase monotonically but retain the same shape up to a filler loading of 20 vol %, with a noticeable change in the terminal slope for the 30 vol % filled sample. This change in the relaxation spectrum of the blends is consistent with the discontinuity in the T_g values obtained from DSC (Table 5). There is also evidence of failure of time-temperature superposition (TTS) at low frequencies for the 30 vol % filled sample. Zero-shear-rate viscosities were calculated from the relation

$$\eta_0 = \lim_{\omega \rightarrow 0} \left(\frac{G''}{\omega} \right) \quad (4)$$

and are reported in Table 5.²⁹ It is also evident from Figure 7a that the addition of POSS filler results in an additional, volume-fraction-dependent shift in the linear viscoelastic properties of these filled materials. The

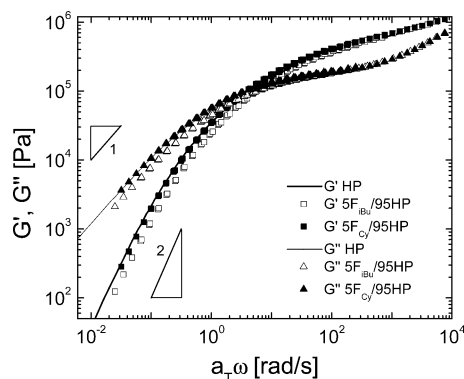


Figure 8. Master curves for the storage and loss moduli of three different samples: PMMA homopolymer, PMMA homopolymer containing 5 vol % cyclohexyl-POSS, and PMMA homopolymer containing 5 vol % isobutyl-POSS ($T_0 = 190\text{ }^{\circ}\text{C}$).

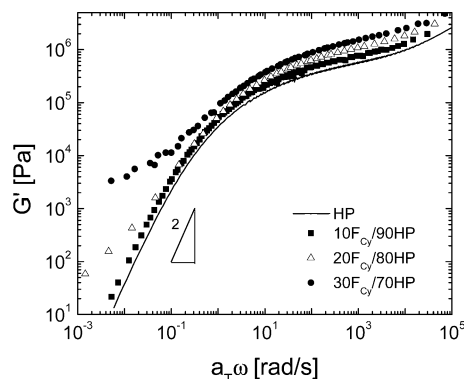


Figure 9. Master curves for the storage modulus of PMMA filled with between 0 and 30 vol % cyclohexyl-POSS ($T_0 = 190\text{ }^{\circ}\text{C}$).

curves can thus be shifted by additional factors (a_ϕ , b_ϕ) to generate a material master curve, as shown in the inset to Figure 7a. We discuss this further in the Discussion section below.

In Figure 8, we show the linear viscoelastic moduli for the homopolymer HP and two blends of homopolymer with 5 vol % POSS filler (5F_{iBu}/95HP and 5F_{Cy}/95HP) at $T_0 = 190\text{ }^{\circ}\text{C}$. In contrast to the response observed in the filled copolymer, there is very little change in the storage modulus G' or the loss modulus G'' of the 5 vol % cyclohexyl-POSS-filled homopolymer. The curves for the isobutyl-POSS-filled homopolymer exhibit a less-sustained plateau in G' than that observed in either the pure homopolymer or the 5% cyclohexyl-POSS-filled sample, and thus the values of G' and G'' in the terminal region are noticeably lower for the isobutyl-POSS-filled homopolymer. As we discuss further below, the lack of reinforcement of the linear viscoelastic moduli at low loadings is indicative of substantial nanodispersion of the POSS in the PMMA matrix at low volume fractions of filler. This behavior can be contrasted with that shown in Figure 9 for higher volume fractions of cyclohexyl-POSS ($\phi \geq 0.10$) at the same reference temperature $T_0 = 190\text{ }^{\circ}\text{C}$. A substantial increase in G' is seen at these higher loadings, more indicative of conventional rigid filler behavior. The 30 vol % cyclohexyl-POSS-filled data appear to enter a plateau region at frequencies $a_T\omega < 10^{-1}\text{ rad/s}$. The isobutyl-POSS-filled homopolymer system exhibits qualitatively similar behavior at high filler loadings with a less substantial enhancement in the storage modulus. Fu et al.¹⁵ observed similar solidlike behavior at low

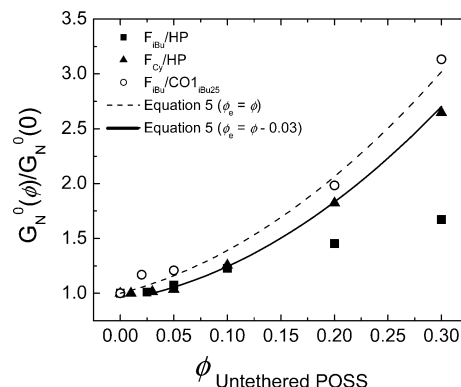


Figure 10. Plateau moduli for blends containing untethered-POSS, $G_N^0(\phi)$, normalized by the respective plateau modulus of the unfilled polymer, $G_N^0(0)$. Data are plotted for PMMA homopolymer filled with both cyclohexyl-POSS and isobutyl-POSS and for isobutyl-POSS in a copolymer containing 25 wt % isobutyl-POSS on the chain (CO1_{iBu25}). The lines represent fits to the Guth–Smallwood equation (eq 5).

frequencies in an ethylene–propylene copolymer filled with comparable amounts of methyl-POSS (20 and 30 wt %). The data in Figure 6 do not extend sufficiently into the terminal flow region (due to thermal degradation) to determine whether secondary plateaus would be present in any of the copolymers; however, the results of Romo-Uribe et al.¹⁰ showed no solidlike behavior at low frequencies for loadings less than 42 wt % tethered-POSS. Thus, it appears that untethered-POSS induces percolation in polymer melts at lower volume fractions than tethered-POSS, which is covalently bound to the entangled matrix.

Discussion

We now seek to understand the systematic trends observed in the thermal and rheological data with respect to the triangular composition diagram in Figure 1. First, in the inset of Figure 6a we show a general trend of increasing entanglement molecular weight M_e with increasing POSS content based on plateau modulus values for the isobutyl-POSS copolymers CO1_{iBu15} and CO2_{iBu25}. This trend is consistent with the results of Romo-Uribe et al.,¹⁰ who showed that tethered-POSS substantially decreases the zero-shear-rate viscosity of weakly entangled polymers at a given molecular weight. This suggests that tethered-POSS, due to its compact size ($d \sim 1.5\text{ nm}$) and relatively small molecular weight ($M_{\text{POSS}} \sim 1000\text{ g/mol}$), reduces the entanglement density in a manner that is analogous to short-chain branches in branched polymers.³⁰ In addition to reducing the linear viscoelastic moduli, tethered-POSS also shifts the curves to higher frequencies (shorter times), thereby accelerating chain relaxation processes.

In Figure 10, we show the variation in the plateau modulus values $G_N^0(\phi)$ [normalized by the homopolymer's plateau modulus $G_N^0(0)$], calculated using eq 2, for all three blend systems. For the two filled homopolymer systems an essentially constant plateau modulus persists at low volume fractions of filler ($\phi \leq 0.05$) before an upturn appears at higher loadings. The values of the plateau moduli at higher loadings are greater for the cyclohexyl-POSS-filled homopolymer than in the equivalent isobutyl-POSS-filled homopolymer blends. The values are also compared to predictions for hard-sphere fillers from the Guth–Smallwood equation:³¹

$$G_N^0(\phi) = G_N^0(0)\{1 + 2.5\phi + 14.1\phi^2\} \quad (5)$$

Although the data show similar trends with respect to eq 5, it is clear that the degree of enhancement is very sensitive to the chemical interaction between the pendant R group and the PMMA matrix. Specifically, a superb fit was obtained for the cyclohexyl-POSS-filled homopolymer system by defining an effective volume fraction to be $\phi_e = \phi - 0.03$. Thus, the first 3 vol % of filler appears to have no apparent effect on the plateau modulus, and above 3 vol % the filler behaves as a hard sphere. From Figure 2a it is clear that there is some cyclohexyl-POSS crystallinity even at a loading of 1 vol %; however, the nanodispersed portion of the filler at loadings $\phi \leq 0.05$ softens the matrix to offset the reinforcement by the crystallites. The filled copolymer system ($F_{iBu}/CO1_{iBu25}$) exhibits a more conventional behavior, showing a monotonic increase in G_N^0 for all loadings. Thus, the copolymer experiences a hard-sphere-like reinforcement when filled with untethered-POSS particles.

In Figure 11, we plot the normalized zero-shear-rate viscosities [$\eta_0(\phi)/\eta_0(0)$] for the blends in an analogous fashion to the plateau moduli in Figure 10. The filled homopolymer systems show an initial *decrease* in the zero-shear-rate viscosity at loadings less than 5 vol %. This result is significantly different from the prediction of the Einstein–Batchelor equation for hard-sphere suspensions (shown by the dotted line in Figure 12):³²

$$\eta_0(\phi) = \eta_0(0)\{1 + 2.5\phi + 6.2\phi^2 + \dots\} \quad (6)$$

which predicts a monotonic increase in viscosity with increasing particle loading. A decrease in viscosity with particle loading has recently been shown in polystyrene melts filled with 5 nm cross-linked polystyrene particles by Mackay et al.,¹⁷ however, no clear trend in viscosity with increasing particle loading was apparent. The present data show a well-defined upward curvature to the viscosity-filler loading curve for the filled homopolymer. For comparison, data from Poslinski et al.³³ for a glass-bead-filled thermoplastic are plotted in Figure 11. The lowest loading investigated by Poslinski et al. ($\phi \sim 0.12$) is close to the prediction of eq 6, but the points at higher loading diverge upward from the curve. The data for the filled homopolymer blends (F_{Cy}/HP and F_{iBu}/HP) would likely show the same diverging behavior at moderate to high filler loadings; however, neither linear viscoelastic nor viscometric tests were able to obtain zero-shear-rate viscosities for loadings above 10 vol %.

The decrease in viscosity at low loadings in the homopolymer blends and the eventual increase at higher loadings are again consistent with the combined presence of nanodispersed filler and crystallites. Initially an appreciable fraction of the POSS particles enter the matrix as amorphous, molecularly dispersed particles, and the remaining fraction forms crystalline aggregates. The nanodispersed particles act as a plasticizer, increasing the free volume due to the local mobility of the pendant R-groups and thereby decreasing the viscosity of the blend, but at higher loadings ($\phi \geq 0.05$) a saturation limit is reached regardless of compounding history. At this point any additional POSS filler agglomerates into crystallites, which increase the viscosity in a way analogous to hard spheres.

By contrast, the filled-copolymer blend system ($F_{iBu}/CO1_{iBu25}$) shows a substantial increase in the zero-

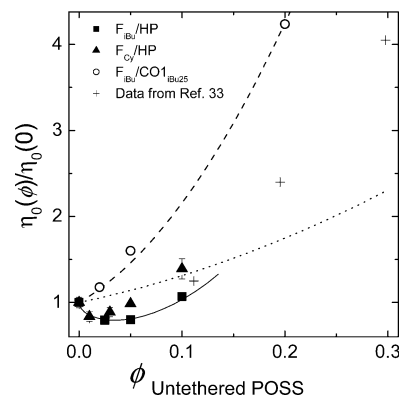


Figure 11. Zero-shear-rate viscosities for blends containing untethered-POSS, $\eta_0(\phi)$, normalized by the respective viscosity of the unfilled polymer, $\eta_0(0)$. Data are plotted for PMMA homopolymer filled with both cyclohexyl- and isobutyl-POSS and for isobutyl-POSS in a copolymer containing 25 wt % isobutyl-POSS on the chain ($CO1_{iBu25}$). The dotted line represents the prediction of the Einstein–Batchelor equation (eq 6), while the dashed line is a plot of eq 6 for an effective volume fraction 2.75 times that of the actual filler value.

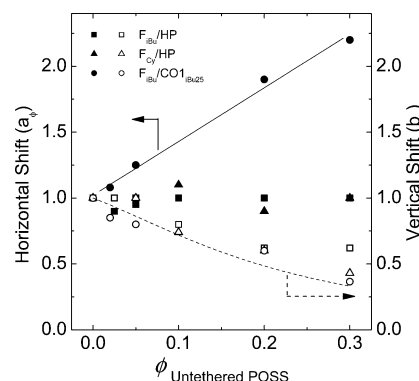


Figure 12. Horizontal (filled symbols) and vertical (open symbols) concentration shift factors for the three blend systems obtained by shifting the storage modulus curves downward and, if necessary, to the left or right onto the respective master curve of the unfilled polymer.

shear-rate viscosity for all loadings (Figure 11). This enhancement is significantly greater than that predicted by eq 6. However, an excellent fit is obtained if the effective volume fraction occupied by a POSS filler cage in the melt is allowed to exceed the actual volume fraction by a factor $\phi_e = 2.75\phi$ (indicated by the dashed line in Figure 11). This result is not surprising when one considers that, in the blend of 5% isobutyl-POSS with the copolymer ($5F_{iBu}/CO1_{iBu25}$), the mole ratio of untethered-POSS groups to tethered-POSS groups ($N_{untethered}/N_{tethered}$) is only 0.23 (see Table 5), meaning the untethered-POSS filler constitutes only 19% of the total POSS contained in the blend. Therefore, the untethered-POSS is able to strongly associate with the tethered-POSS and increase the effective volume fraction of the filler, especially at low filler loadings. This internal amplification of the “effective matrix–filler interaction” leads to the factor of 2.75 multiplying the volume fraction in fitting the data to eq 6.

To further illustrate the differences between the two types of blend systems, both horizontal and vertical concentration shift factors (a_ϕ and b_ϕ , respectively) were computed by shifting the master curves for the storage moduli of the blend samples onto the respective master curve of the unfilled polymer to generate a reduced modulus $G_r'(\omega_r) = b_\phi G'(a_\phi a_T \omega)$ with $b_\phi \leq 1$ and $a_\phi \geq 0.9$

for $\phi > 0$. Similar concentration-dependent shift factors have been used in the construction of universal master curves of semidilute and concentrated polymer solutions.^{34,35} The strong self-similarity of the material functions and the quality of the shifts for the filled copolymer system are shown in the inset to Figure 7a. In Figure 12, we plot the horizontal shift factors a_ϕ (filled symbols) and the vertical shift factors b_ϕ (open symbols) for both the filled homopolymer and the filled copolymer blend systems. No vertical shifts b_ϕ are required in the filled homopolymer blends for $\phi \leq 0.05$; however, the filled copolymer blends require vertical shifts at all filler loadings in order to superpose onto the master curve of the unfilled polymer. The reciprocal of the Guth–Smallwood equation is plotted as the dashed line in Figure 13 to show that the vertical shifts correspond well with the plateau modulus values in Figure 10. All blends above $\phi = 0.05$ require significant vertical shifts, and thus the trend of increasing vertical shifts with filler loading is similar in the filled homopolymer blends and the filled copolymer blends. The behavior of the horizontal shift factors a_ϕ , however, is distinctly different between the two types of blend systems. Only minimal horizontal shifting is required in the filled homopolymer blend systems, whereas in the filled copolymer a linear increase in a_ϕ with a slope of 7.5 is observed with increasing filler content. Thus, for every 13 vol % of untethered-POSS added to the copolymer a subsequent 1 decade increase in relaxation time is observed.

It is helpful at this point to utilize the Doi–Edwards scaling relation for the viscosity of unfilled, entangled polymers:³⁶

$$\eta_0 \cong G_N^0 \tau_{\text{rep}} \quad (7a)$$

where τ_{rep} is the reptation time of the unfilled polymer melt. This scaling relation may be altered to describe a filled polymer by writing

$$\eta_0 = G_N^0(\phi) \tau_{\text{rep}}(\phi) = \left(\frac{G_N^0}{b_\phi} \right) (\tau_{\text{rep}} a_\phi) \quad (7b)$$

where a_ϕ and b_ϕ are the same concentration shift factors plotted in Figure 12. To a first approximation, filler particles may be expected to reinforce a polymer melt, which leads to the factor $1/b_\phi$ in the modulus term of eq 7b, or to retard chain motions, which leads to the term a_ϕ in the reptation term of eq 7b. Overall, the reinforcement is more substantial in the filled copolymer systems (see Figure 10), but both types of blend systems show a significant reinforcement effect which closely follows the prediction of the Guth–Smallwood equation (eq 5). The reptation term, which is directly related to the horizontal shift factor a_ϕ , is not significantly affected in the untethered-POSS–homopolymer blend systems, but it linearly increases with filler loading in the copolymer blends. The rheological data in Figure 6 for unfilled copolymers show clearly that tethered-POSS, in the absence of untethered-POSS filler, does not retard chain relaxation processes and in fact speeds them up (i.e., “plasticizes” them) relative to the homopolymer. Thus, the additional slowdown in the dynamics of the filled copolymer reflected in the term $a_\phi > 1$ must be due to thermodynamic associations between tethered-POSS cages on the chain and untethered-POSS particles in

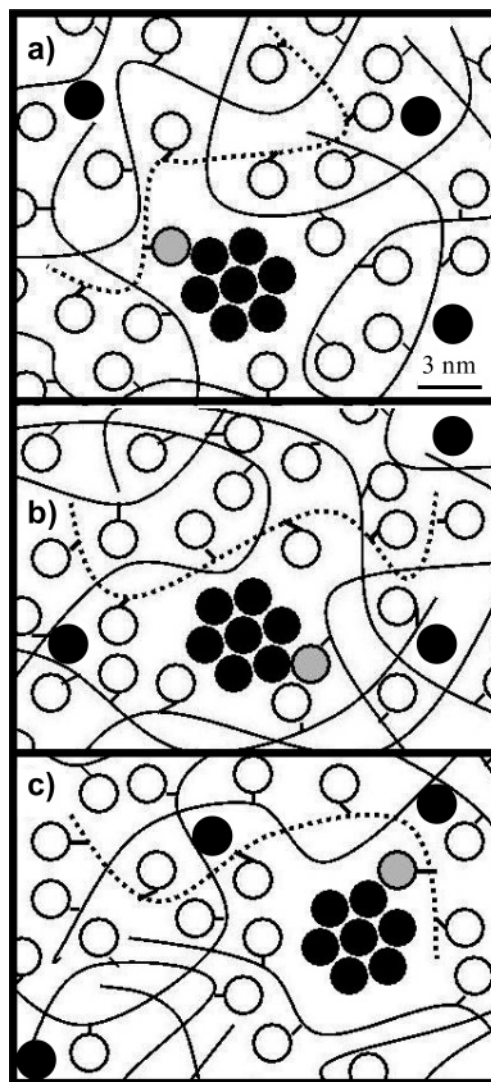


Figure 13. Schematic of the filled copolymer blend ($F_{iBu}/CO1_{iBu25}$). At low loadings of untethered-POSS (black circles), most of the tethered-POSS groups are present in an unbound state (open circles). However, a kinetic exchange takes place whereby a particular chain (represented by the dashed line) may contain (a) an “active” tethered-POSS group (gray circle) which forms a thermodynamic association with a nanocrystallite of untethered-POSS. This temporary association may (b) break, thus allowing the chain to reptate freely before (c) a different tethered-POSS group on the same chain forms an association with the nanocrystallite. This kinetic exchange between an associated and a dissociated state leads to the dramatic slowdown in the relaxation processes in the copolymer matrix.

the blend. This is the principal effect responsible for the large increase in the zero-shear-rate viscosity shown in Figure 11.

This combination of a retardation in the relaxation processes and an enhancement in the modulus in a well-entangled melt can be described by kinetic models such as the “sticky reptation” model of Liebler et al.³⁷ It has been previously conjectured by Romo-Uribe et al.¹⁰ that this model and other mechanisms are important in POSS-containing copolymers; however, our results strongly indicate that it is the addition of POSS filler to a POSS-containing copolymer that results in the retardation, not simply the incorporation of tethered-POSS into a polymer chain. The horizontal shift factor a_ϕ is primarily related to the “stickiness” of the chains, which is characterized by the number of “stickers” (in

this case, the number of tethered-POSS groups on the chain), the average lifetime for a sticker in the associated state, and the average fraction of stickers which are in the associated state, which is a function of both the tethered-POSS content and the untethered-POSS content. The filled homopolymer system experiences no significant horizontal shifts over the range of loadings examined because the chains contain no sticky groups. In the filled copolymer system, however, the sticky groups constitute 25 wt % of the polymer chains and lead to a rapid increase in relaxation time with particle loading. The vertical shift factor b_ϕ is also affected by the concentration of sticky groups on the chain, but it is affected by inert, rigid particles as well and thus a substantial increase in the plateau modulus G_N^0 with filler loading is present in both types of blend systems.

An unusual aspect of the linear viscoelastic results for the filled copolymer system is that the storage and loss moduli G' and G'' show virtually no change in shape up to 20 vol % filler loading (Figure 7). In other filled systems with attractive matrix–filler interactions such as carbon-black-filled elastomers,³⁸ silica-filled poly(ethylene oxide),¹⁶ and clay-filled polystyrene-*g*-maleic anhydride,³⁹ a sustained plateau in the storage modulus, $G' \geq 10^4$ Pa, typically persists at low frequencies for loadings $\phi \ll 0.20$. This is often attributed to a percolated network caused by substantial chain adsorption onto the filler particles.¹⁶ There is ample evidence from the shape of the linear viscoelastic moduli and the glass transition temperatures indicating that percolation does not occur in the F_{iBu}/CO_{1iBu25} system until 30 vol % isobutyl-POSS filler is added; however, the linear increase in the horizontal shift factor a_ϕ is present at all loadings. This is because the adsorption effect is significantly different in the filled copolymer system of the present study, in which the polymer backbone has no strong attraction to the isobutyl-POSS filler (as evidenced by the plasticization at low loadings in the filled homopolymer). Thus, the only portions of the copolymer chain that experience a thermodynamic attraction to the untethered-POSS are the tethered-POSS groups distributed randomly along the backbone, and though these groups constitute a substantial weight fraction of the copolymer CO_{1iBu25} , they are incorporated in only 3.4 mol % of the repeat units. Thus, only 1 out of approximately every 60 carbon atoms in the copolymer backbone contains a covalently tethered isobutyl-POSS particle, and at low loadings of untethered-POSS, hundreds of backbone carbon atoms will separate the tethered-POSS groups that are actively bound to a crystallite. This indicates that the retardation caused by the associations between the tethered and untethered isobutyl-POSS is a local effect restricted to isolated nanoscopic domains within the sample, rather than being caused by a global percolated network. The schematic in Figure 13 further illustrates this postulate.

In Figure 13a, a reptating copolymer chain (represented by the dashed line) is close enough to a small (~ 5 nm) nanocrystallite of untethered-POSS that one of its tethered-POSS groups (represented by the gray circle) has associated with the crystallite, forming a temporary cross-link. Very soon after (Figure 13b), the bound tethered-POSS cage disassociates from the crystallite, and the copolymer chain is again free to reptate along its contour length; however, before the chain has fully diffused away from the crystallite, a new associa-

tion is formed (Figure 13c), this time with a different tethered-POSS group taking part in the association. Throughout this process the chain has been able to translate its center of mass despite the kinetic exchange between a bound and an unbound state. The associations significantly delay the motion of the chain along its contour length (and thereby increase the reptation time, τ_{rep}); however, they do not significantly alter the mobility of the unbound segments (when the amount of untethered-POSS is small). In addition, the associations are short-lived ($\tau_{assoc} \ll \tau_{rep}$), allowing the shape of the linear viscoelastic moduli to remain the same for filler loadings $\phi \leq 0.20$. At filler loadings $\phi > 0.20$, the probability of a tethered-POSS cage taking part in an association surpasses a critical point, and thereafter significant molecular mobility is lost due to the number of temporary cross-links per molecule. This is responsible for the increase in the glass transition temperature observed in the filled copolymer at 30 vol % filler (Table 5). Furthermore, at this point the untethered-POSS becomes the dominant POSS species in the system, and the tethered-POSS groups become saturated in their nanoscopic associations with untethered-POSS. This leads to the formation of large numbers of crystallites that percolate throughout the PMMA matrix.

Time–Temperature Superposition. The addition of unbound POSS nanofiller into an entangled polymer matrix may result in several competing effects. The high local mobility of the pendant R groups on the Si_3O_{12} cages will create additional free volume and thus locally plasticize the matrix, leading to enhanced molecular mobility; conversely, the addition of a rigid filler (albeit nanoscale in characteristic dimension) is expected to result in enhanced local dissipation with a less clear effect on free volume. The TTS shift factors obtained experimentally were analyzed using the WLF framework⁴⁰ to further investigate the effect of POSS filler on free volume in the blends.

The time–temperature shift factors $a_T(T, T_0)$ used in constructing Figures 6–12 were obtained by shifting $\tan \delta$ curves obtained over a range of test temperatures to a reference temperature ($T_0 = 190$ °C for the homopolymer, $T_0 = 135$ °C for the copolymer). To illustrate the quality of the TTS, an example of original data is given in Figure 14. In Figure 14a we plot the unshifted $\tan \delta$ curves for the 10 vol % cyclohexyl-POSS–homopolymer blend, and in Figure 14b we show the curves after shifting. No vertical shifting was required.

Initially, $\log a_T$ was plotted against the reciprocal of the absolute temperature to determine whether the rheology of the samples followed Arrhenius behavior; however, high correlation coefficients were only obtained at high temperatures ($T \geq 190$ °C). Therefore, the WLF equation was employed in order to capture the temperature dependence of the shift factors over the entire temperature range.⁴⁰

$$\log a_T = \frac{-c_1^0(T - T_0)}{c_2^0 + (T - T_0)} \quad (8)$$

WLF coefficients were determined by plotting the quantity $-(T - T_0)/\log a_T$ against $(T - T_0)$;⁴⁰ the coefficient c_1^0 was obtained from the reciprocal of the slope and the coefficient c_2^0 from the intercept. An example of the use of this method can be found in the work of Fetters et al. for polyisobutylene melts.⁴¹ Values

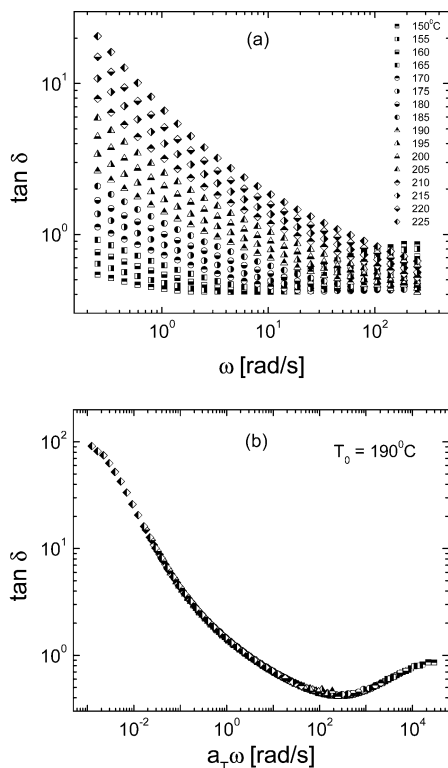


Figure 14. Loss tangent ($\tan \delta = G''/G'$) curves for PMMA filled with 10 vol % cyclohexyl-POSS: (a) unshifted frequency sweeps at different temperatures; (b) all curves shifted to a reference temperature of $T_0 = 190^\circ\text{C}$.

of the WLF coefficients are reported in Table 4 for all filler–homopolymer blends. The value of $c_1^0 = 8.6$ obtained for the PMMA homopolymer agrees well with values reported by Fuchs et al. for PMMA homopolymers ($8.6 \leq c_1^0 \leq 9.4$)²⁸ at the same reference temperature $T_0 = 190^\circ\text{C}$.

A representative WLF plot for the cyclohexyl-POSS–homopolymer blend system is shown in Figure 15a, one set of data corresponding to the unfilled homopolymer and another for a blend containing 10 vol % cyclohexyl-POSS. There is a small but reproducible difference in the slope and the y-intercept of the two lines, indicating differences in the respective WLF coefficients. The c_1^0 values can be related to the fractional free volume f_0 using the relation³⁷

$$f_0 = \frac{B}{2.303c_1^0} \quad (9)$$

where B is a constant usually assumed to be unity. Values of f_0/B are reported in Table 4 along with the zero-shear-rate viscosities for the homopolymer blends. Surprisingly, for filler loadings $\phi \leq 0.05$, the value of the fractional free volume of the unfilled homopolymer obtained from TTS ($f_0/B = 0.050$) is larger than that of the cyclohexyl-POSS–homopolymer system (0.048) but smaller than that of the isobutyl-POSS–homopolymer system (0.051–0.052). The difficulty in developing clear trends lies in the above-mentioned competition between molecular dispersion and crystalline aggregation, which is present at all loadings (see Figure 2a). The decrease in viscosity seen at low loadings in the filler–homopolymer system is almost certainly a result of additional free volume generated by the dispersed POSS nanoparticles, whose mobile, pendant R groups are expected to create

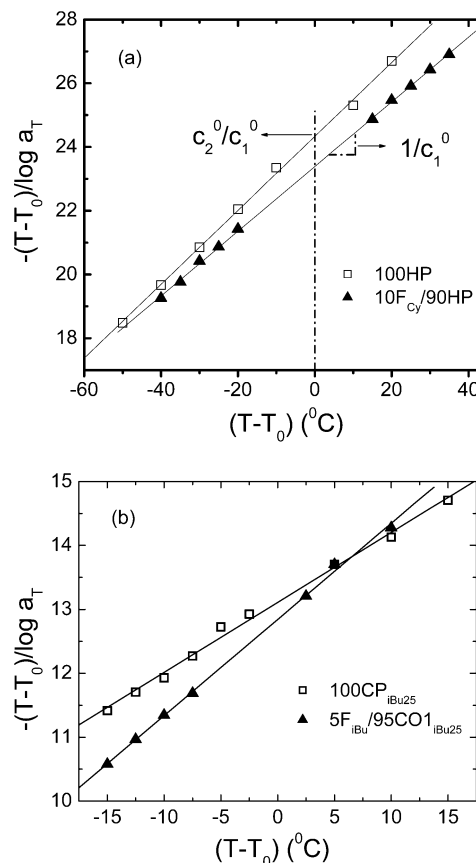


Figure 15. WLF plots for (a) unfilled PMMA homopolymer and homopolymer containing 10 vol % cyclohexyl-POSS ($T_0 = 190^\circ\text{C}$) and (b) unfilled copolymer containing 25 wt % isobutyl-POSS on the chain and respective copolymer containing 5 vol % isobutyl-POSS filler ($T_0 = 135^\circ\text{C}$).

appreciable void space; the WLF coefficients in the F_{Cy}/HP system do not support this trend because of the complication caused by the crystallites, which reinforce the melt and thereby skew the WLF coefficients to values which suggest an opposing trend. The effect of the crystallites can be demonstrated by analyzing the coefficients obtained in the F_{Cy}/HP system. Up to 10 vol % cyclohexyl-POSS filler, the first WLF coefficient shows a monotonic increase from $c_1^0 = 8.6$ for the homopolymer to $c_1^0 = 9.9$ for the 10% filled sample. But the 20% filled sample has a c_1^0 value of only 7.6, substantially smaller than the homopolymer's value, which leads to a higher calculated fractional free volume value ($f_0/B = 0.057$). Nothing in the linear viscoelastic data in Figure 9 or in the T_g values in Table 4 predicts such a change in molecular arrangement. Future rheological studies on a POSS-filled system in which crystallization is entirely absent or at least greatly suppressed would help to clarify the interesting role of molecularly dispersed POSS on the thermorheological properties.

In Figure 15b, we show the WLF plot for the unfilled copolymer and the copolymer filled with 5 vol % isobutyl-POSS filler. Addition of untethered-POSS clearly has a stronger effect at low loadings ($\phi \leq 0.05$) on the time–temperature behavior in the copolymer blends. The slope of the $5F_{iBu}/95CO1_{iBu25}$ line is notably larger, leading to smaller c_1^0 and c_2^0 values. The WLF coefficients for the filled copolymer system are reported in Table 5. In the range of isobutyl-POSS loadings $0.02 \leq \phi \leq 0.20$, increasing the amount of POSS filler increases both the fractional free volume f_0 and the zero-shear-

rate viscosity η_0 . In particular, at loadings of $\phi \leq 0.05$, which contain only small amounts of crystallite content (see Figure 2b), the fractional free volume increases from $f_0/B = 0.048$ for the unfilled copolymer at $T_0 = 135$ °C to $f_0/B = 0.065$ for the copolymer blended with 5 vol % isobutyl-POSS. That the free volume and viscosity should both increase concomitantly is counter to the concepts introduced by Doolittle which relate free volume in liquids to viscosity.⁴² However, our result is not unreasonable, as the thermodynamic attraction between the well-dispersed isobutyl-POSS filler and the tethered-isobutyl-POSS groups in the copolymer chain could offset the increase in free volume observed in the system. The significant nanodispersion of the untethered-POSS in the copolymer system, evidenced by both the X-ray pattern for the 5F_{iBu}/95CO_{1-iBu} blend in Figure 2b and the strong retardation of chain motion evident from the linear viscoelastic data, is responsible for the observed increase in free volume.

Conclusions

Poly(methyl methacrylate)s containing both tethered and untethered polyhedral oligomeric silsesquioxanes (POSS) were investigated using wide-angle X-ray diffraction, differential scanning calorimetry, and rheological characterization. Entangled linear copolymers containing covalently-tethered-POSS showed a decrease in the plateau modulus compared to the homopolymer, and this trend was nearly the same for two 25 wt % POSS copolymers with different organic R groups. This behavior was attributed to the tethered-POSS behaving analogously to a short-chain branch, thereby reducing the entanglement density and softening the polymer in the melt state.

When untethered-POSS was blended with PMMA homopolymer, wide-angle X-ray diffraction (WAXD) showed significant crystallinity of untethered-POSS even at loadings as low as 1 vol %, while significant crystallinity in the filled copolymer blends was not observed until greater than 5 vol % filler had been added. Melting endotherms from DSC suggest a regime at low loadings ($\phi \leq 0.05$) in which a large fraction of untethered-POSS enters the homopolymer in an amorphous state before a solubility limit is reached, at which point virtually all additional POSS filler is incorporated into crystallites.

Contrasting behavior was observed between the rheology of untethered-POSS-homopolymer blends and the untethered-POSS-copolymer blends. A minimum in the zero-shear-rate viscosity and a constant plateau modulus at loadings below 5 vol % were seen for both the isobutyl-POSS-filled and the cyclohexyl-POSS-filled homopolymer, indicating an initial plasticization of the matrix by the untethered POSS filler. However, at higher loadings these values increased in a way consistent with hard-sphere fillers. Combining the thermal and rheological data leads to the conclusion that untethered-POSS distributes in two ways in a homopolymer matrix: as nanoscopically dispersed particles and as crystallites. The copolymer blends showed a substantial increase in viscosity at all loadings. This was attributed to a substantial retardation of chain relaxation processes caused by significant association between the POSS cages on the chains and those in the blend. This thermodynamic attraction is particularly effective at retarding chain motions in nanoscopic domains while still allowing macroscopic relaxation of the sample.

Time-temperature superposition (TTS) was used to determine whether the decrease in viscosity in the untethered-POSS-homopolymer blends could be correlated with an increase in free volume. Linear regression fits to the WLF equation were excellent; however, there was no strong trend in the coefficients for the homopolymer blends. This was due to the POSS filler's tendency to form crystallites, which became dominant at filler loadings above 5 vol %. The untethered-POSS-copolymer blend system shows a significant decrease in the WLF coefficients upon the addition of small amounts of untethered-POSS filler, suggesting an increase in free volume with filler loading. Surprisingly, the viscosity also increases dramatically in this region; however, this counterintuitive result can be explained by the strong thermodynamic interaction between tethered and untethered-POSS moieties, which more than offsets the plasticization caused by the free volume increase.

Acknowledgment. This research was sponsored by the DURINT project of the U.S. Air Force under Grant F49620-01-1-0447. Special thanks are given to Joe Adario and Peter Kloumann of the X-ray Characterization Lab at MIT's Center for Materials Science and Engineering. The use of the experimental facilities at MIT's Institute for Soldier Nanotechnologies is also greatly appreciated.

References and Notes

- (1) POSS is a trademark of Hybrid Plastics (www.hybridplastics.com).
- (2) Lichtenhan, J. D.; Vu, N. Q.; Carter, J. A.; Gilman, J. W.; Feher, F. J. *Macromolecules* **1993**, *26*, 2141.
- (3) Schwab, J. J.; Lichtenhan, J. D. *Appl. Organomet. Chem.* **1998**, *12*, 707.
- (4) Lucke, S.; Stoppek-Langner, K. *Appl. Surf. Sci.* **1999**, *145*, 713.
- (5) Li, G. Z.; Wang, L. C.; Ni, H. L.; Pittman, C. U. *J. Inorg. Organomet. Polym.* **2001**, *11*, 123.
- (6) Zheng, L.; Farris, R. J.; Coughlin, E. B. *Macromolecules* **2001**, *34*, 8034.
- (7) Mather, P. T.; Jeon, H. G.; Romo-Uribe, A.; Haddad, T. S.; Lichtenhan, J. D. *Macromolecules* **1999**, *32*, 1194.
- (8) Xu, H. Y.; Kuo, S. W.; Chang, F. C. *Polym. Bull. (Berlin)* **2002**, *48*, 469.
- (9) Xu, H. Y.; Kuo, S. W.; Lee, J. S.; Chang, F. C. *Macromolecules* **2002**, *35*, 8788.
- (10) Romo-Uribe, A.; Mather, P. T.; Haddad, T. S.; Lichtenhan, J. D. *J. Polym. Sci., Part B: Polym. Phys.* **1998**, *36*, 1857.
- (11) Zhang, W. H.; Fu, B. X.; Seo, Y.; Schrag, E.; Hsiao, B.; Mather, P. T.; Yang, N. L.; Xu, D. Y.; Ade, H.; Rafailovich, M.; Sokolov, J. *Macromolecules* **2002**, *35*, 8029.
- (12) Blanski, R. L.; Phillips, S. H.; Chaffee, K.; Lichtenhan, J.; Lee, A.; Geng, H. P. *Polym. Prepr.* **2000**, *41*, 585.
- (13) Zheng, L.; Waddon, A. J.; Farris, R. J.; Coughlin, E. B. *Macromolecules* **2002**, *35*, 2375.
- (14) Vaia, R. A.; Giannelis, E. P. *MRS Bull.* **2001**, *26*, 394.
- (15) Fu, B. X.; Gelfar, M. Y.; Hsiao, B. S.; Phillips, S.; Viers, B.; Blanski, R.; Ruth, P. *Polymer* **2003**, *44*, 1499.
- (16) Zhang, Q.; Archer, L. A. *Langmuir* **2002**, *18*, 10435.
- (17) Mackay, M. E.; Dao, T. T.; Tuteja, A.; Ho, D. L.; Van Horn, B.; Kim, H. C.; Hawker, C. J. *Nature Mater.* **2003**, *2*, 762.
- (18) Einstein, A. *Ann. Phys. (Leipzig)* **1906**, *19*, 371.
- (19) Glotzer, S. C. *Nature Mater.* **2003**, *2*, 713.
- (20) (a) Brown Jr., J. F.; Vogt Jr., L. H. *J. Am. Chem. Soc.* **1965**, *87*, 4313. (b) Feher, F. J.; Newman, D. A.; Walzer, J. F. *J. Am. Chem. Soc.* **1989**, *111*, 1741. (c) Feher, F. J.; Budzichowski, T. A.; Blanski, R. L.; Weller, K. L.; Ziller, J. W. *Organometallics* **1991**, *10*, 2526. (d) Feher, F. J.; Terroba, R.; Ziller, J. W. *Chem. Commun.* **1999**, *22*, 2309.
- (21) Barry, A. J.; Daudt, W. H.; Domicone, J. J.; Gilkey, J. W. *J. Am. Chem. Soc.* **1955**, *77*, 4248.
- (22) Larsson, K. *Ark. Kemi* **1960**, *16*, 209. For (*n*-propyl)-POSS, two crystal forms are present, and the densities for these are 1.09 and 1.20 g/cm³. For isopropyl-POSS, a density of 1.20 g/cm³ was given, and for (*n*-butyl)-POSS a crystal density of

- 1.14 g/cm³ was reported. These data suggest that isobutyl-POSS should have a density at least as high as that of (*n*-butyl)-POSS. However, as is shown in the Results section, isobutyl-POSS has two crystal structures, which, if similar to (*n*-propyl)-POSS, would have different but similar densities. An estimate of 1.15 g/cm³ was thus taken as a reasonable median value for the density of the isobutyl-POSS filler.
- (23) Kong, X.; Tang, B. Z. *Chem. Mater.* **1998**, *10*, 3352.
 - (24) (a) Kanazawa, A.; Tsutsumi, O.; Ikeda, T.; Nagase, Y. *J. Am. Chem. Soc.* **1997**, *119*, 7670. (b) Sudholter, E. J. R.; Engberts, J. B. F. N.; de Jeu, W. H. *J. Phys. Chem.* **1982**, *86*, 1908. (c) Busico, V.; Corradini, P.; Vacatello, M. *J. Phys. Chem.* **1982**, *86*, 1033.
 - (25) Wu, S. J. *J. Polym. Sci., Part B: Polym. Phys.* **1989**, *27*, 723.
 - (26) Lomellini, P.; Lavagnini, L. *Rheol. Acta* **1992**, *31*, 175.
 - (27) Larson, R. G. *The Structure and Rheology of Complex Fluids*; Oxford University Press: New York, 1998.
 - (28) Fuchs, K.; Friedrich, C.; Weese, J. *Macromolecules* **1996**, *29*, 5893.
 - (29) The five lowest-frequency points in G'' were used to determine η_0 for each blend sample. The average slope of $\log G''$ vs $\log \omega$ in the terminal region for the PMMA blends with reported viscosities was 0.997 ± 0.011 .
 - (30) Dealy, J. M.; Wissbrun, K. F. *Melt Rheology and Its Role in Plastics Processing*; Von Nostrand Reinhold: New York, 1990.
 - (31) Smallwood, H. M. *J. Appl. Phys.* **1944**, *15*, 758.
 - (32) (a) Batchelor, G. K. *J. Fluid Mech.* **1970**, *41*, 545. (b) Batchelor, G. K. *J. Fluid Mech.* **1971**, *46*, 813. (c) Batchelor, G. K. *J. Fluid Mech.* **1977**, *83*, 97.
 - (33) Poslinski, A. J.; Ryan, M. E.; Gupta, R. K.; Seshadri, S. G.; Frechette, F. J. *J. Rheol.* **1988**, *32*, 703.
 - (34) Graessley, W. W. *Adv. Polym. Sci.* **1974**, *16*, 133.
 - (35) Nakajima, N.; Varkey, J. P. *J. Appl. Polym. Sci.* **1998**, *69*, 1727.
 - (36) Doi, M.; Edwards, S. F. *The Theory of Polymer Dynamics*; Clarendon Press: Oxford, 1986.
 - (37) Liebler, L.; Rubinstein, M.; Colby, R. H. *Macromolecules* **1991**, *24*, 4701.
 - (38) Yurekli, K.; Krishnamoorti, R.; Tse, M. F.; McElrath, K. O.; Tsou, A. H.; Wang, H.-C. *J. Polym. Sci., Part B: Polym. Phys.* **2000**, *39*, 256.
 - (39) Lim, Y. T.; Park, O. O. *Rheol. Acta* **2001**, *40*, 220.
 - (40) Ferry, J. D. *Viscoelastic Properties of Polymers*, 3rd ed.; John Wiley & Sons: New York, 1980.
 - (41) Fetters, L. J.; Graessley, W. W.; Kiss, A. D. *Macromolecules* **1991**, *11*, 3136.
 - (42) Doolittle, A. K.; Doolittle, D. B. *J. Appl. Phys.* **1957**, *28*, 901.

MA048934L